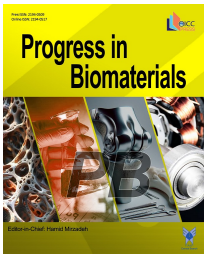

Volume 13, Issue 4, 132415 (1-10)

Progress in Biomaterials (PIBM)

https://doi.org/10.57647/pibm.2024.132415

Structure-Driven pH-Responsive Doxorubicin Release from Titanium-Modified Zeolite Nanoparticles

Fatemeh Mirjalili*

Department of Materials Engineering, May.C., Islamic Azad University, Maybod, Iran.

***Corresponding author:** f.mirjalili1404@iau.ir

Original Research

Abstract:

In this study, nanozeolite powders were synthesized via a chemical route using zeolite soil, sodium silicate, sodium hydroxide, calcined kaolin, and distilled water. The influence of synthesis parameters, particularly stirring time, on crystal growth and structural evolution was systematically investigated. Subsequently, the synthesized zeolite powders were surface-modified with controlled amounts of titanium nanoparticles through continuous magnetic stirring for 24 h to tailor their physicochemical properties.Crystallite size analysis based on Scherrer's equation and field emission scanning electron microscopy (FESEM) revealed that increasing the titanium nanoparticle content led to a significant reduction in average grain size, while prolonged stirring time promoted crystal growth. The crystallite sizes obtained from X-ray diffraction (XRD) analysis were in good agreement with FESEM observations, confirming the reliability of the structural characterization. Titanium modification induced pronounced grain refinement and increased surface reactivity without altering the fundamental aluminosilicate framework of the zeolite.The drug delivery performance of the prepared nanozeolites was evaluated using doxorubicin (DOX) as a model anticancer drug. In vitro release studies conducted at pH 7.4 and pH 5.5 demonstrated a clear pH-responsive release behavior, with significantly enhanced DOX release under acidic conditions mimicking the tumor microenvironment. Titanium-modified nanozeolites exhibited higher DOX loading capacity and more controlled release profiles compared to unmodified samples, attributed to increased surface hydroxyl groups and refined microstructure.Overall, the results highlight that, controlled synthesis and titanium surface modification effectively enhance the structural and functional performance of nanozeolites, making them promising candidates for pH-triggered and targeted anticancer drug delivery applications.

Keywords:

Nanozeolite; XRD; FE-SEM; Doxorubicin; Hydroxyl groups; DOX release

Cite this article: Mirjalili, F. Structure-Driven pH-Responsive Doxorubicin Release from Titanium-Modified Zeolite Nanoparticles. *Progress in Biomaterials* **13**(4), Article 15 (2024).

1. Introduction

Cancer remains one of the leading causes of mortality worldwide, and despite substantial progress in chemotherapy, conventional treatment strategies are often limited by nonspecific drug distribution, systemic toxicity, and severe side effects. Widely used chemotherapeutic agents, such as doxorubicin (DOX), cisplatin, methotrexate, and paclitaxel, exhibit high therapeutic efficacy; however, their narrow therapeutic windows highlight the urgent need for advanced drug delivery systems that can enhance therapeutic outcomes while minimizing adverse effects (Edis et al., 2021). Zeolites are crystalline hydrated aluminosilicates characterized by well-defined microporous frameworks and exchangeable cations (Na^+, K^+, Mg^{2+}, Ca^{2+}), which allow reversible adsorption of water and high loading of therapeutic molecules without significant structural alteration (Ansari et al., 2013). First identified by Cronstedt in 1756, the name "zeolite" is derived from the Greek words zein (to boil) and lithos (stone), referring to the effervescence observed upon heating due to water release (Marlina and Ginting, 2015; Ahmedzeki et al., 2016). Among naturally occurring zeolites, clinoptilolite and stilbite are the most widely studied, although over 85 natural types and numerous synthetic analogues are now recognized (Sharma et al., 2008). Owing to their exceptional ion-exchange capacity, adsorption behavior, and catalytic activity, zeolites have been extensively utilized in industrial applications, including molecular sieves, catalysts, and adsorbents (Edis et al., 2021; Alvarez-Ayuso et al., 2003; Zhang et al., 2011; Hisham et al., 2011). Despite their advantages, conventional zeolites often face limitations, such as restricted pore size, low channel interconnectivity, and limited affinity for

anionic species, which frequently necessitate functional modification (Maretto et al., 2014; Ordou and Fathizadeh, 2011; Holmberg et al., 2003). Nanostructuring of zeolites overcomes these constraints by increasing external surface area, enhancing surface reactivity, and shortening diffusion pathways, resulting in improved adsorption, catalytic efficiency, and biocompatibility (Toshev and Valitechev, 2005; Htay and Mya, 2008; Nik and Alias, 2007; Rahman et al., 2012; Nabiollah et al., 2013; Mendoza-Castro et al., 2023; Yaneri and Petit, 2013). Moreover, surface modification with surfactants or metal nanoparticles, such as zinc or titanium, has been reported to further enhance functional performance, including catalytic activity and antibacterial properties (Bina et al., 2012; Rostami et al., 2012; Nisi and Babai, 2014; Naeej et al., 2012; Son et al., 2023; Mosavi Fard et al., 2013). The use of inexpensive natural precursors, such as kaolin, allows scalable and cost-effective synthesis for both industrial and biomedical applications (Mirjalili et al., 2022; Hao et al., 2021). Doxorubicin (DOX) is a widely used anthracycline chemotherapeutic agent for the treatment of a broad range of solid tumors and hematological malignancies. However, the clinical effectiveness of doxorubicin is significantly limited by severe dose-dependent side effects, particularly cardiotoxicity, as well as poor tumor selectivity and rapid systemic distribution (Edis et al., 2021). These drawbacks necessitate the development of advanced drug delivery systems capable of enhancing tumor-specific accumulation while minimizing systemic toxicity. Recent studies have demonstrated that nanozeolites and zeolitic imidazolate frameworks (ZIFs) are promising carriers for anticancer drugs, particularly DOX.

Their porous structure and high surface area enable efficient drug loading, while surface modification facilitates pH-responsive release in acidic tumor microenvironments, enhancing cellular uptake and reducing systemic toxicity (Liquan et al., 2023; Chen et al., 2007; DeFrates et al., 2022). Although TiO_2-modified zeolites and other clay-based nanocarriers have been previously reported, most studies rely on post-synthesis coating or impregnation. In this work, zeolite nanoparticle formation and titanium surface modification were integrated during synthesis, allowing better control of crystal size, morphology, and surface properties. This strategy produced titanium-modified nanozeolites with improved drug-loading capacity, tunable pH-responsive release, and favorable biocompatibility. Zeolite nanoparticles synthesized via this approach were systematically evaluated as nanocarriers for doxorubicin (DOX) delivery, focusing on structure–property relationships, drug-loading efficiency, pH-triggered release, and potential biomedical applicability.

2. Materials and methods

The materials used in this study included sodium silicate (Germany) containing 10% NaOH and 27% SiO_2 as the silica source, and sodium hydroxide (Merck, Germany, 98% purity) to provide an alkaline medium for zeolite synthesis. Kaolin (Abtin Chemical Co., Iran), a fine natural aluminosilicate powder, was used as the primary precursor. Titanium nanoparticles (Merck, Germany, 98% purity) were employed for surface modification of the zeolite nanoparticles, and high-purity natural zeolite soil was obtained from Nikan Company (Iran). For drug delivery studies, doxorubicin hydrochloride (DOX, Sigma-Aldrich, USA) was used as the model anticancer drug. Phosphate-buffered saline (PBS, pH 7.4) was applied for drug loading and release experiments, and simulated body fluid (SBF) was used for *in vitro* biomineralization assessments. For cytotoxicity evaluation, Dulbecco's Modified Eagle Medium (DMEM) supplemented with 10% fetal bovine serum (FBS) and antibiotics, along with MTT reagent (Sigma-Aldrich, USA), were employed. Additional analytical-grade chemicals, including hydrochloric acid, calcium chloride, sodium sulfate, potassium chloride, potassium hydrogen phosphate trihydrate, and magnesium chloride hexahydrate, were used for the preparation of simulated body fluid and buffering solutions.

2.1 Synthesis of zeolite nanoparticles

Approximately 500 g of natural zeolite soil was initially calcined at 680 °C for 3 h in a muffle furnace to remove moisture, organic matter, and other volatile components. Calcined kaolin and sodium silicate were used as primary silica and aluminosilicate sources, while sodium hydroxide served to adjust the alkalinity. The raw materials were accurately weighed using an analytical balance ($\pm$0.01 g) and mixed with distilled water to prepare a homogeneous slurry.Additionally, the general procedures for weighing and mixing of raw materials are not described here, as they follow standard experimental protocols reported elsewhere (Nisi and Babai, 2014; Mirjalili et al., 2022). For samples B2–B4, an identical precursor composition was employed, while the stirring time was systematically varied to investigate its effect on crystal growth. The mixtures were stirred for 12 h (B2), 24 h (B3), and 36 h (B4). After stirring, all samples were dried at 100 °C for 3 days, washed with distilled water until the pH reached approximately 10, filtered, and finally dried at 100 °C for 12 h. The obtained powders were subsequently used for surface modification.

2.2 Surface modification of zeolite nanoparticles

To modify the zeolite surfaces, 1 g of each synthesized sample was dispersed in distilled water, and titanium nanoparticles were added according to the solid compositions listed in Table 1, corresponding to a fixed TiO_2 content of 35 wt.% relative to the zeolite mass. The suspensions were stirred for 24 h to ensure uniform surface modification. The modified samples were then filtered, dried at 120 °C for 1 h, and calcined at 500 °C for 2 h to improve nanoparticle adhesion and structural stability.

2.3 Preparation for drug loading and release

Titanium-modified zeolite nanoparticles were dispersed in phosphate-buffered saline (PBS, pH 7.4) for drug-loading experiments. Doxorubicin hydrochloride (DOX, Sigma-Aldrich, USA) was added to the suspension under gentle stirring at room temperature and incubated for 12 h to achieve maximum adsorption onto the nanoparticle surfaces. The drug-loaded nanocomposites were then separated by filtration or centrifugation, washed with PBS to remove un-

Table 1. Formulation of samples.

Sample	Nano zeolite (g)	Nano titanium oxid (g)	Water (cc)	Stirring time (h)
C1	1	0.35	10	12
C2	1	0.35	10	24
C3	1	0.35	10	36

bound DOX, and freeze-dried.In vitro drug release studies were performed in PBS (pH 7.4) and acetate buffer (pH 5.5) at 37 °C to simulate physiological and tumor microenvironments. The release profiles were monitored over time using UV-Vis spectrophotometry, enabling evaluation of pH-responsive release behavior and potential for targeted anticancer therapy.

2.4 Characterization techniques

The structural, morphological, and surface properties of the synthesized and titanium-modified zeolites were characterized using complementary techniques. X-ray diffraction (XRD, Bruker D8 Advance, Cu Kα, $\lambda = 1.5406$ Å, $2\theta = 5° - 70°$, 2°/min) was used to identify crystalline phases, assess titanium-induced changes, and estimate crystallite size via the Scherrer equation. Particle morphology and titanium distribution were examined by field emition scanning electron microscopy (FE-SEM, JEOL JSM-6510LV). Surface area, pore volume, and pore size distribution were determined from N_2 adsorption–desorption isotherms using a Micromeritics ASAP 2020 (BET method). FTIR spectra (Thermo Nicolet iS50, $4000 - 400$ cm^{-1}) provided information on functional groups, bonding interactions, and potential DOX loading sites. Particle size and surface charge in aqueous suspension were measured using a Malvern Zetasizer Nano ZS. DOX loading and release were quantified by UV–Vis spectrophotometry (Shimadzu 160A) in PBS (pH 7.4) and acetate buffer (pH 5.5). Biocompatibility and anticancer efficacy were evaluated via MTT assays on MCF-7 and normal fibroblast cells after $24 - 72$ h of treatment with varying nanoparticle concentrations.

3. Results and discussion

3.1 Particle size, surface charge, and implications for drug loading

Dynamic light scattering (DLS) analysis was performed to evaluate the hydrodynamic diameter, size distribution, and surface charge of the titanium-modified zeolite nanoparticles. All samples exhibited narrow size distributions, with polydispersity index (PDI) values ranging from 0.16 to 0.21, indicating good colloidal stability. The average hydrodynamic diameters decreased slightly with increasing stirring time during synthesis: 142 ± 5 nm for B2-Ti (12 h), 135 ± 4 nm for B3-Ti (24 h), and 128 ± 3 nm for B4-Ti (36 h). This trend suggests that longer stirring promotes more uniform dispersion and reduces nanoparticle agglomeration.Zeta potential measurements revealed negative surface charges for all samples, ranging from -28 ± 2 mV (B2-Ti) to -33 ± 2 mV (B4-Ti). The increasing magnitude of negative zeta potential with stirring time indicates enhanced electrostatic stability, which is favorable for maintaining dispersion in aqueous media and for subsequent drug adsorption.The hydrodynamic diameter, polydispersity index (PDI), zeta potential, and doxorubicin (DOX) loading efficiency of the titanium-modified zeolite nanoparticles are summarized in Table 2. The observed particle size and surface charge characteristics directly influenced the loading efficiency of doxorubicin (DOX). Smaller and more uniformly dispersed nanoparticles exhibited higher surface area and stronger electrostatic interactions with the cationic DOX molecules, resulting in enhanced drug loading. Furthermore, the negative surface charge contributes to pH-responsive drug release, as protonation in acidic tumor-like environments promotes DOX desorption, supporting controlled and targeted anticancer therapy. These results confirm that titanium-modified nanozeolites synthesized under optimized stirring conditions possess suitable physicochemical properties for effective drug delivery applications.

3.2 X-ray diffraction (XRD) results

Figure 1(a) presents the X-ray diffraction (XRD) patterns of samples B1 and B2, prepared with different amounts of water, sodium hydroxide, and sodium silicate with a stirring time of 12 h, and samples B2, B3, and B4 prepared with the same composition but varying stirring times of 12, 24, and 36 h, respectively.

Table 2. Hydrodynamic diameter, polydispersity index, zeta potential, and DOX loading of titanium-modified zeolite nanoparticles.

Sample	Hydrodynamic diameter (nm)	Polydispersity index (PDI)	Zeta Potential (mV)	DOX loading efficiency (%)
B2-Ti (12 h stirring)	142 ± 5	0.21	-28 ± 2	62 ± 3
B3-Ti (24 h stirring)	135 ± 4	0.18	-31 ± 3	68 ± 2
B4-Ti (36 h stirring)	128 ± 3	0.16	-33 ± 2	74 ± 3

The XRD patterns of all B samples exhibit characteristic reflections of a crystalline zeolite structure, confirming uniform nanoparticle formation. No additional peaks corresponding to secondary phases were observed, and the positions of the main diffraction peaks remained essentially unchanged, suggesting consistent crystallization across all samples. Comparing B1 and B2, increasing the amount of water and precursors prolonged the synthesis, leading to larger crystallite sizes (10.2 nm for B1 versus 14 nm for B2, calculated using the Scherrer equation), consistent with Mosavi Fard et al. (2013). B2 and B3 exhibited similar crystallite sizes, while extending the stirring time from 12 h (B2) to 36 h (B4) slightly increased the crystallite size to 14.8 nm due to reduced nucleation and enhanced crystal growth.For titanium-modified samples C1–C3, the zeolite crystalline structure was retained, with no additional peaks indicating secondary phases. The incorporation of TiO_2 nanoparticles slightly decreased crystallite size relative to the corresponding B samples and enhanced structural ordering, consistent with the effects of surface modifiers on montmorillonite microstructure reported by Mirjalili et al. (2022). The diffraction peak at $\sim 2\theta \approx 25°$ corresponds to the (101) plane of anatase TiO_2, confirming the presence of TiO_2) (Song et al., 2024). The XRD results of the synthesized zeolite-based nanocarriers provide a clear structural basis for interpreting their doxorubicin (DOX) release behavior. All B and titanium-modified C samples exhibited a single crystalline phase with no detectable secondary phases, indicating structural stability and uniformity, which are essential for predictable and controlled drug release (Hao et al., 2021; DeFrates et al., 2022). The relatively small crystallite sizes ($\approx 10-15$ nm, Scherrer equation) afford a high surface-to-volume ratio and abundant microporous channels, facilitating efficient DOX loading via physical adsorption and electrostatic interactions. Gradual increases in crystallite size with longer stirring times (B2–B4) suggest enhanced crystallinity and reduced defect density, which limit rapid diffusion and produce a more sustained release profile, whereas smaller crystallites with higher defect density (B1) promote faster initial release due to shorter diffusion pathways. For titanium-modified samples (C1–C3), the original zeolite framework was retained, with no new phases observed, confirming that ,TiO_2 incorporation occurs mainly at the surface. The slight reduction in crystallite size and increased surface heterogeneity introduce additional active sites, enhancing DOX–carrier interactions through hydrogen bonding and coordination effects. Consequently, titanium-modified nanozeolites exhibited improved drug retention, reduced burst release, and tunable pH-responsive release behavior, consistent with reports on metal-modified zeolite and clay-based carriers (Alshawwa et al., 2022). Overall, these findings demonstrate that controlled crystallite size, preserved crystallinity, and tailored surface chemistry collectively enable sustained and predictable DOX delivery, highlighting the potential of titanium-modified nanozeolites as efficient inorganic drug carriers.

3.3 BET surface area and porosity analysis

Nitrogen adsorption–desorption analysis revealed that all synthesized samples exhibit type IV isotherms with H3 hysteresis loops, confirming mesoporous structures formed by aggregated zeolite nanoparticles. For the unmodified B-series, the BET-specific surface area decreased with increasing crystallite size and stirring time, consistent with XRD and DLS results. Sample B1, with the smallest crystallite size ($\sim$ 10.2 nm), showed the highest surface area (412 m^2/g), total pore volume of 0.46 cm^3/g, and an average pore diameter of 4.5 nm. In contrast, B2–B4 displayed gradually reduced surface areas ($358-305$ m^2/g) and pore volumes ($0.41-0.36$ cm^3/g) as crystallites grew, reflecting enhanced crystal growth and decreased accessible porosity (Rosas-Arbelaez and Fijneman, 2020; Derakhshankhah et al., 2020; Ojo et al., 2020). Titanium-modified samples (C1–C3) exhibited slightly lower BET surface areas ($254-298$ m^2/g) due to partial pore blocking by TiO_2nanoparticles, while maintaining high total pore volumes ($0.29-0.33$ cm^3/g) and slightly increased average pore diameters ($5.0-5.4$ nm). The presence of TiO_2 introduces additional polar sites and hydroxyl groups, enhancing hydrogen bonding and electrostatic interactions with doxorubicin (DOX). Consequently, titanium-modified zeolites demonstrated improved DOX retention, reduced burst release, and sustained diffusion-controlled kinetics, despite their lower surface area. These results underscore the critical balance between porosity and surface chemistry in designing zeolite-based nanocarriers for controlled and pH-responsive anticancer drug delivery (Liang-Peng et al., 2009; Song et al., 2024; Alshawwa et al., 2022).

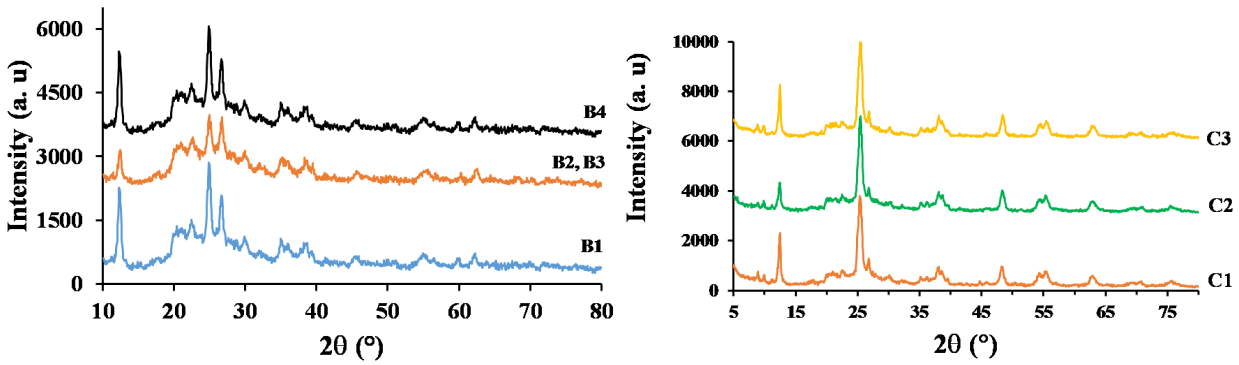

Figure 1. (a): X-ray diffraction pattern of samples B1, B2, B3, B4, (b): X-ray diffraction pattern of samples C1, C2, C3.

3.4 FTIR analysis

The FTIR spectra of zeolite samples B1–B4, synthesized with varying amounts of water, sodium hydroxide, sodium silicate, and heating durations (12 – 36 h), were recorded over 350 – 3850 cm^{-1} (Fig. 2) and display characteristic vibrational features of zeolitic frameworks, confirming the formation of crystalline aluminosilicate structures. Broad bands at 3435 – 3442 cm^{-1} correspond to stretching vibrations of hydroxyl (–OH) groups, while bands at 1637 – 1641 cm^{-1} are due to bending vibrations of adsorbed water within zeolite channels. The intense band at 1034 – 1103 cm^{-1} is attributed to internal asymmetric stretching of Si–O–T (T = Si or Al), reflecting a well-developed tetrahedral network (Liang-Peng et al., 2009; Song et al., 2024). Minor shifts and intensity variations indicate subtle effects of precursor composition and heating time on local bonding without altering the fundamental framework. Additional bands at 792 – 794 cm^{-1} and 695 – 697 cm^{-1} correspond to external Si–O–T and Si–O–Al stretching, respectively, while bands at 533 – 539 cm^{-1} and 470 – 489 cm^{-1} are related to lattice vibrations and TO_4 bending modes (Jansson et al., 2015; Kamegawa et al., 2014). These features confirm aluminum incorporation and the presence of negatively charged sites suitable for DOX adsorption. Following titanium modification, the characteristic zeolitic bands were preserved, with broadening and increased intensity in the hydroxyl region (3435 – 3442 cm^{-1}) indicating enhanced surface –OH density, associated with TiO_2 nanoparticles on the zeolite surface. The TiO_2 modification improves hydrophilicity and provides additional adsorption sites for DOX, promoting stronger interactions and more controlled release profiles. Titanium modification of zeolite surfaces enhances interactions with doxorubicin (DOX) compared to unmodified aluminosilicate interfaces. The presence of TiO_2 nanoparticles introduces additional surface hydroxyl groups, enabling stronger hydrogen bonding, electrostatic attraction, and surface complexation with DOX molecules. This effect is particularly pronounced in samples with refined grain sizes, where the increased surface-to-volume ratio amplifies Ti-related surface functionalities, resulting in higher drug loading efficiency and more controlled release.Titanium incorporation also governs pH-responsive DOX release. Under physiological conditions (pH 7.4), strong interactions between DOX and Ti–OH/Si–OH groups stabilize the drug within the zeolite matrix, slowing release. In acidic conditions (pH 5.5), protonation of DOX weakens these interactions, facilitating desorption and accelerated release, consistent with experimental observations. In addition to these chemical effects, microstructural refinement induced by titanium contributes to controlled diffusion, further enhancing release tunability. Overall, FTIR and structural analyses confirm that titanium modification improves the functional performance of zeolite nanocarriers without altering the fundamental aluminosilicate framework. By increasing surface hydroxyl density and refining particle morphology, TiO_2-modified zeolites provide an optimized platform for efficient DOX loading and pH-triggered release, highlighting their potential as advanced carriers for targeted anticancer therapy.

3.5 Field emission scanning electron microscopy (FE-SEM) results

FESEM images of samples B1-B4 are presented in Fig. 3(a). Increasing the amounts of water, NaOH, and Na_2SiO_3 (B1 → B2) led to larger grain sizes. Prolonged heating (B2 → B4) further promoted grain growth, resulting in even larger grains. The average grain sizes derived from FESEM images are summarized in Table 3. These observations can be attributed to enhanced grain growth and coalescence. Sample B4 exhibited the most uniform grain distribution and the lowest porosity. FESEM-derived grain sizes were in good agreement with crystallite sizes calculated from X-ray diffraction using the Scherrer equation, though FESEM grains are larger as they represent aggregates of multiple crystallites.To examine the effect of titanium nanoparticles, samples C1–C3 were prepared by incorporating 0.35 wt.%

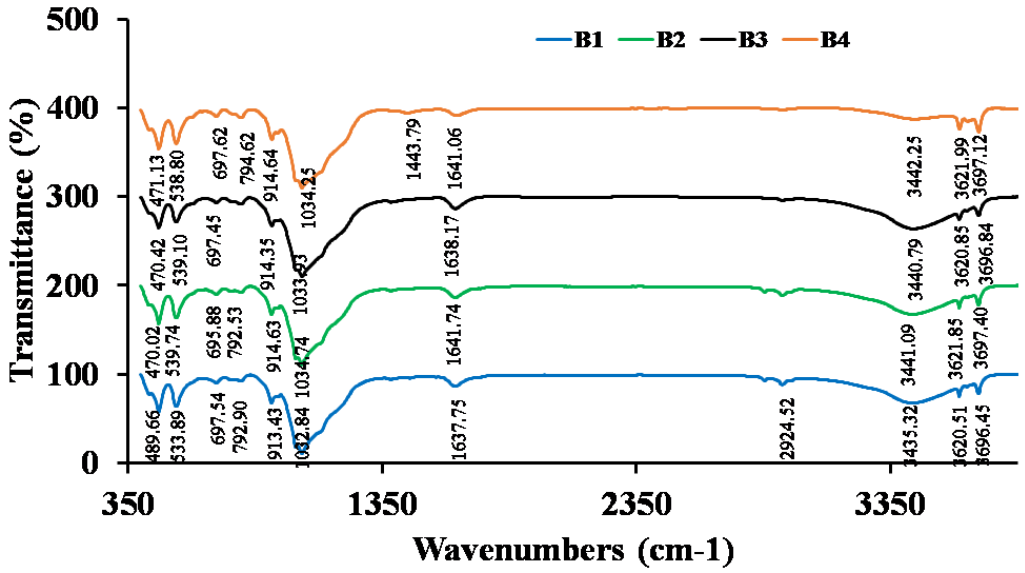

Figure 2. FTIR results of samples B1, B2, B3, B4.

TiO_2 into B2–B4, respectively. FESEM images in Fig. 3(b) show a significant reduction in grain size: 40.52 nm (C1), 33.82 nm (C2), and 36.69 nm (C3), although the distribution is less uniform due to nanoparticle agglomeration. Compared with the corresponding base samples, the reductions were 21% (B2 → C1), 49.5% (B3 → C2), and 27.6% (B4 → C3), with the largest decrease observed in C2. These results indicate that Ti nanoparticles effectively refine grains, particularly in the sample derived from B3, consistent with previous findings on montmorillonite modification (Mirjalili et al., 2022). Grain refinement induced by titanium nanoparticles increases the specific surface area, potentially enhancing drug–surface interactions. However, nanoparticle agglomeration and structural heterogeneity create tortuous diffusion pathways, which can mitigate burst release and promote sustained drug release. Titanium-based nanocarriers, including TiO_2 structures, have previously exhibited pH-dependent controlled release of doxorubicin, where stronger interactions between the drug and carrier surface, or confinement within nanoscale features, reduce burst release and maintain cumulative release over extended periods (Derakhshankhah et al., 2020).

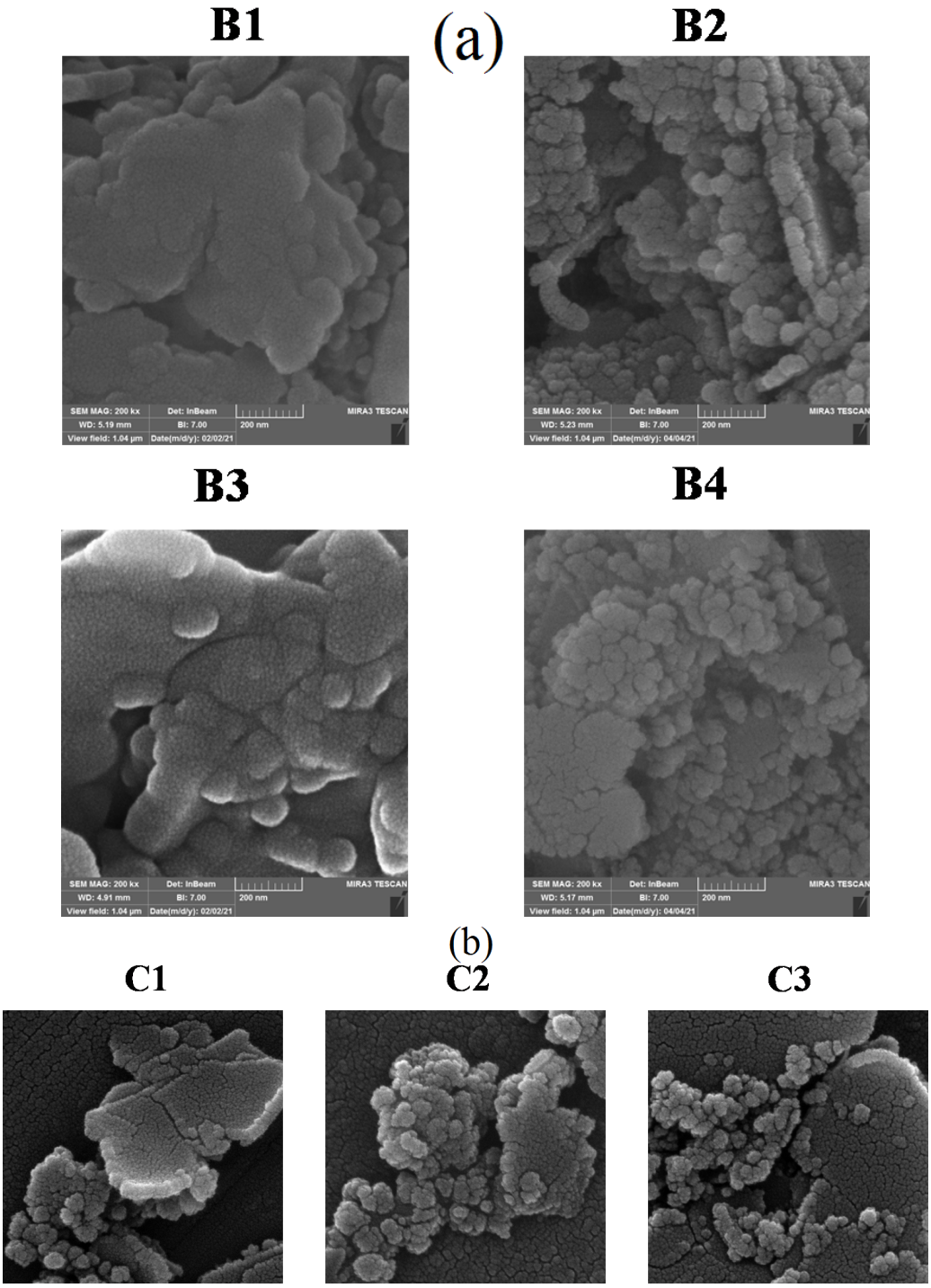

Figure 3. (a): FESEM images of samples B1, B2, B3, B4, (b): FESEM images of samples C1, C2, C3.

Table 3. Grain sizes obtained from different samples by FESEM images.

Sample	B1	B2	B3	B4	C1	C2	C3
Average grain size (nm)	32.46	46.51	67.06	56.02	36.69	33.82	40.52

Similarly, montmorillonite-containing nanocomposites have been widely studied for doxorubicin delivery, where the presence of clay layers increases adsorption sites, reducing the initial release fraction while prolonging overall release (Mirjalili et al., 2022). In the present composites, although the finer grain size of C2 could theoretically enhance early drug–surface contact, the observed nanoparticle agglomeration and complex microstructure likely create tortuous diffusion channels that favor controlled release. This balance between increased surface area and morphological heterogeneity aligns with prior studies emphasizing that surface area enhancement must be carefully managed to achieve sustained doxorubicin release (Lu et al., 2023). Collectively, these results suggest that titanium nanoparticle-induced grain refinement and the associated microstructural evolution significantly influence doxorubicin release kinetics, with C2 demonstrating the most pronounced effect on sustained release behavior, consistent with previously reported mechanisms in TiO_2 and montmorillonite-based drug carriers.

3.6 *In vitro* drug release

The *in vitro* cumulative release profiles of doxorubicin (DOX) from all investigated samples demonstrated pronounced pH-responsive behavior (Fig. 4). Under acidic conditions (pH 5.5), simulating the tumor microenvironment and endo/lysosomal compartments, DOX release was significantly higher than at physiological pH (7.4), enabling preferential drug delivery at tumor sites while minimizing premature leakage. At pH 7.4, cumulative release after 48 h ranged from $38 \pm 2\%$ to $51 \pm 3\%$ for B2-Ti, B3-Ti, and B4-Ti, whereas at pH 5.5, release increased to $62 \pm 3\%$, $68 \pm 3\%$, and $74 \pm 3\%$, respectively. The enhanced release under acidic conditions is attributed to protonation of DOX, weakening electrostatic interactions with the negatively charged zeolite framework and facilitating desorption. A clear correlation between release behavior, particle size, and surface charge was observed. Dynamic light scattering (DLS) and zeta potential analyses indicated that smaller nanoparticles with more negative surface charges, particularly B4-Ti, exhibited higher DOX loading and faster release under acidic conditions, due to increased surface area and more accessible adsorption sites. Titanium modification not only enhanced DOX loading but also improved release tunability; partial nanoparticle agglomeration in some Ti-modified samples created tortuous diffusion pathways, suppressing burst release and promoting sustained delivery. These results confirm that, TiO_2-modified nanozeolites combine pH-triggered responsiveness with controlled release kinetics, providing an effective platform for targeted anticancer therapy. Controlled particle size, surface charge, and TiO_2 incorporation are critical for optimizing drug–carrier interactions and achieving efficient, tumor-targeted DOX delivery (Mu et al., 2021).

3.6.1 Drug release kinetics

To elucidate the mechanism governing doxorubicin (DOX) release from the synthesized zeolite-based nanocarriers, the experimental release data were fitted to commonly used kinetic models, including the zero-order, first-order, Higuchi, and Korsmeyer–Peppas models. Among these, the Higuchi and Korsmeyer–Peppas models provided the best correlation coefficients (R^2), indicating that DOX release from both unmodified and titanium-modified nanozeolites is predominantly diffusion-controlled (Vy Anh and Sang-Wha, 2021). For unmodified B-series samples, the release pro-

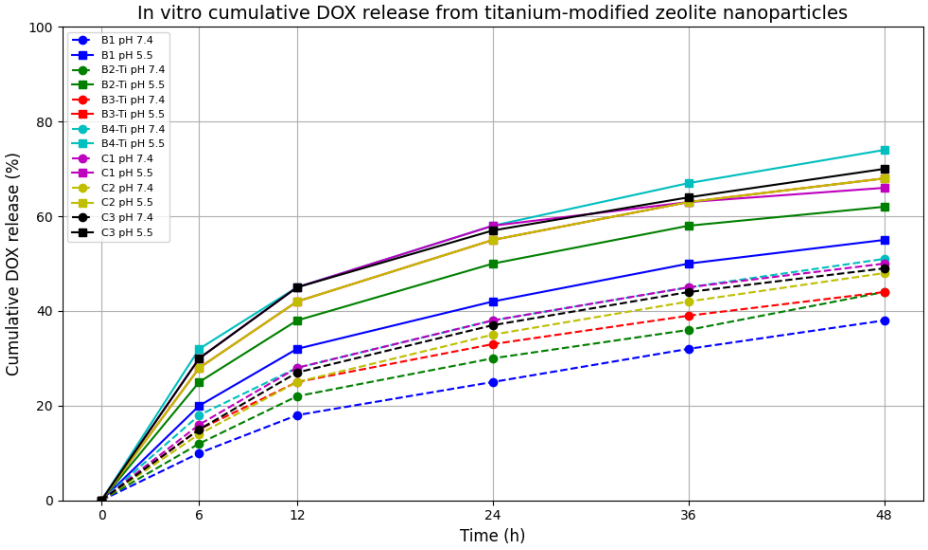

Figure 4. *In vitro* cumulative DOXrelease from titanium modified zeolite nano particles.

files closely followed the Higuchi model, suggesting that DOX diffusion through the porous zeolite network is the dominant release mechanism. The relatively faster release observed in samples with smaller crystallite size (e.g., B1) can be attributed to higher surface area and shorter diffusion paths, which facilitate rapid migration of drug molecules from surface-accessible pores into the surrounding medium. This observation is consistent with reports on inorganic porous nanocarriers, where reduced crystallinity and increased surface defects promote diffusion-driven release behavior (Ojo et al., 2020). In contrast, titanium-modified samples (C1–C3) exhibited release behavior better described by the Korsmeyer–Peppas model, with diffusion exponent (n) values in the range of $0.45 - 0.60$. These values indicate anomalous (non-Fickian) transport, suggesting that DOX release is governed by a combination of diffusion and strong drug–carrier interactions. The introduction of titanium nanoparticles increases surface polarity and enhances electrostatic and hydrogen-bonding interactions between DOX molecules and the aluminosilicate framework, thereby retarding drug diffusion and suppressing the initial burst release. Similar kinetic behavior has been reported for metal-modified zeolite and clay-based drug delivery systems designed for sustained anticancer therapy (Dos Reis et al., 2021). Furthermore, prolonged rotation time during synthesis resulted in slightly increased crystallite size and improved structural ordering, which translated into lower release rate constants. This trend confirms that increased crystallinity reduces pore accessibility and diffusion rates, leading to more sustained release profiles. The absence of zero-order kinetics indicates that the release is not governed by matrix erosion but rather by diffusion through a stable inorganic framework, which is desirable for long-term drug delivery applications. Overall, the kinetic analysis confirms that DOX release from the developed nanozeolites is primarily diffusion-controlled, with titanium surface modification effectively shifting the release mechanism toward anomalous transport and sustained release. These findings, in agreement with recent studies on inorganic nanocarriers, demonstrate that precise control of crystallite size and surface chemistry is a key factor in tailoring drug release kinetics for anticancer applications.

3.7 *In vitro* cytotoxicity evaluation by MTT assay

The *in vitro* cytotoxicity of base (B1–B4) and titanium-modified (C1–C3) zeolite nanoparticles loaded with doxorubicin (DOX) was evaluated using the MTT assay, a standard colorimetric method for assessing cell metabolic activity and viability via mitochondrial dehydrogenase activity (Mosmann, 1983). The base samples exhibited relatively high cell viability across all tested concentrations and incubation periods, reflecting their larger particle sizes, lower specific surface areas, and slower DOX release rates. Limited intracellular drug availability in these samples resulted in weaker cytotoxic effects. A gradual decrease in viability from B1 to B4 corresponded to reduced particle size, enhanced surface area, and increased DOX release and cellular uptake (Danaei et al., 2018; Pandya et al., 2024). In contrast, titanium-modified nanocomposites demonstrated markedly higher cytotoxicity than their base counterparts. Grain refinement induced by TiO_2 incorporation increased surface area and DOX loading, facilitating more efficient interaction with cancer cells. Nanoparticles of this size are preferentially internalized via endocytosis, resulting in elevated intracellular drug concentrations and improved anticancer efficacy (Shi et al., 2017). Among the modified samples, C1 exhibited a rapid initial reduction in cell viability, consistent with its faster DOX release, whereas C2 showed moderate early-stage cytotoxicity followed by sustained viability reduction over time. This behavior is likely related to partial nanoparticle agglomeration, which increases diffusion tortuosity, suppresses burst release, and prolongs drug exposure, a desirable feature for reducing acute systemic toxicity while maintaining long-term therapeutic effects (Mingxia et al., 2021; Li et al., 2017). The observed cytotoxicity profiles correlate well with the pH-responsive release behavior, where enhanced DOX release under acidic conditions-mimicking the tumor microenvironment and intracellular compartments-leads to selective cancer cell killing while preserving normal cell viability (Ziental et al., 2020; Minotti et al., 2004). Overall, MTT results confirm that titanium modification optimizes the interplay between nanoparticle microstructure, release kinetics, and biological response. Among all samples, C2 displayed the most favorable cytotoxicity profile, balancing controlled initial toxicity with sustained cell killing, highlighting TiO_2-modified nanozeolites as promising platforms for targeted and safer DOX delivery in cancer therapy.

4. Conclusion

In conclusion, zeolite nanoparticles were successfully synthesized via a chemical route, producing uniformly crystalline structures with tunable crystallite sizes. Systematic adjustment of reagent concentrations and stirring times enabled controlled grain growth, with crystallite sizes ranging from 10.2 to 14.8 nm and improved morphological uniformity in sample B4. Titanium surface modification further refined the particle size, with sample C2 showing the most pronounced reduction ($\sim 49.5\%$), while simultaneously increasing surface area and creating diffusion-controlled pathways advantageous for functional applications. These structural enhancements translated directly into superior drug delivery performance. TiO_2-modified zeolite nanoparticles exhibited pH-responsive doxorubicin release, achieving higher release under acidic conditions mimicking the tumor microenvironment, while maintaining controlled desorption and minimizing burst release. Reduced particle size and surface modification contributed to increased drug loading and improved release tunability. Overall, the study demonstrates that, precise control of synthesis parameters combined with titanium surface modification offers a robust strategy to engineer zeolite-based nanocarriers with optimized structural and functional properties. Beyond conventional catalytic and adsorption uses, these TiO_2-modified nanozeolites show strong potential as smart, pH-sensitive platforms for targeted anticancer therapy with reduced systemic toxicity.

Availability of data and materials
The datasets generated during and/or analyzed during the current study are available from the corresponding author on reasonable request.

Conflict of interests
The authors declare that they have no known competing financial interests or personal relationships that could have appeared to influence the work reported in this paper.

References

Ahmedzeki S., Yilmaz S., Ban A. (2016) Synthesis and characterization of nanocrystalline zeolite Y. *Al-Khwarizmi Engineering Journal* 12 (1): 79–89.

Alshawwa S. Z., Kassem A. A., Farid R. M., Mostafa S. K., Labib G. S. (2022) Nanocarrier Drug Delivery Systems: Characterization, Limitations, Future Perspectives and Implementation of Artificial Intelligence. *Pharmaceutics* 14 (4): 883. DOI: https://doi.org/10.3390/pharmaceutics14040883.

Alvarez-Ayuso E., Garcia-Sanchez A., Querol X. (2003) Purification of metal electroplating wastewaters using zeolites. *Water Research* 37:4855–4862. DOI: https://doi.org/10.1016/j.watres.2003.08.009.

Ansari M., Aroujalian A., Raisi A., Dabir B., Fathizadeh M. (2013) Preparation and characterization of nano-NaX zeolite by microwave-assisted hydrothermal method. *Advanced Powder Technology* 24:1–6. DOI: https://doi.org/10.1016/j.apt.2013.10.021.

Bina B., Abrahimi A., Mohammadi A., Amin H. M. Porzamani (2012) The application of modified nano zeolite with cationic surfactants. *Health System Research* 5:524–533.

Chen X., Qiao M., Xie S., Fan K., Zhou W., He H. (2007) Self-Construction of Core-Shell and Hollow Zeolite Analcime Icositetrahedra: A Reversed Crystal Growth Process via Oriented Aggregation of Nanocrystallites and Recrystallization from Surface to core. *J Am Chem Soc* 129 (43): 13305–12. DOI: https://doi.org/10.1021/ja074834u.

Danaei M., Dehghankhold M., Ataei S., Hasanzadeh Davarani F., Javanmard R., Dokhani A., Khorasani S., Mozafari M. R. (2018) Impact of Particle Size and Polydispersity Index on the Clinical Applications of Lipidic Nanocarrier Systems. *Pharmaceutics* 10:57. DOI: https://doi.org/10.3390/pharmaceutics10020057.

DeFrates K. G., Engström J., Sarma N., Umar A., Shin J., Cheng J., Xie W., Pochan D., Omar A. K., Messersmith P. B. (2022) The influence of molecular design on structure–property relationships of a supramolecular polymer prodrug. Proc. Natl. Acad. Sci. U.S.A. (44): e2208593119. DOI: https://doi.org/10.1073/pnas.2208593119.

Derakhshankhah H., Jafari S., Sarvari S., Barzegari E., Moakedi F., Ghorbani M., Tayebi L. (2020) Biomedical application of Zeolitte nanoparticles with an emphasis on medical interventions. *International Journal of Nanomedicine* 15:363–386. DOI: https://doi.org/10.2147/IJN.S234573.

Dos Reis S. B., Oliveira Silva J. de, Garcia-Fossa F., Leite E. A., Malachias A., Pound-Lana G., Mosqueira V. C. F., Oliveira M. C., Barros A. L. B. de, Jesus M. B. de (2021) Mechanistic insights into the intracellular release of doxorubicin from pH-sensitive liposomes. *Biomedicine & Pharmacotherapy* 134:110952. DOI: https://doi.org/10.1016/j.biopha.2020.110952.

Edis Z., Wang J., Waqas M. K., Ijaz M., Ijaz M. (2021) Nanocarriers-Mediated Drug Delivery Systems for Anticancer Agents: An Overview and Perspectives. *International Journal of Nanomedicine* 16:1313–1330. DOI: https://doi.org/10.2147/IJN.S289443.

Hao J., Stavljenić Milašin I., Batu Eken Z., Mravak-Stipetic M., Pavelić K., Ozer F. (2021) Effects of Zeolite as a Drug Delivery System on Cancer Therapy: A Systematic Review. *Molecules* 26:6196–6229.

Hisham A., Moustafa M., Moustafa E., Abdelrahman E. A. (2011) Synthesis of mordenite zeolite in absence of organic template. *Advanced Powder Technology* 23:757–760.

Holmberg B., Wang J., Norberk J. (2003) Controlling size and yield of zeolite Y nanocrystals using tetramethylammonium bromide. *Microporous and Mesoporous Materials* 59:13–28. DOI: https://doi.org/10.1016/S1387-1811(03)00271-3.

Htay M., Mya O. (2008) Preparation of zeolite Y catalyst for petroleum cracking. *World Academy of Science, Engineering and Technology* 48:114–120. https://api.semanticscholar.org/CorpusID:15935304

Jansson I., Suárez S., Garcia-Garcia F. J., Sánchez B. (2015) Zeolite-TiO_2 hybrid composites for pollutant degradationin gas phase. *Appl. Catal. B Environ* 178:100–107. DOI: https://doi.org/10.1016/j.apcatb.2014.10.022.

Kamegawa T., Ishiguro Y., Kido R., Yamashita H. (2014) Design of composite photocatalyst of TiO_2 and Y-zeolite for degradation of 2-propanol in the gas phase under UV and visible light irradiation. *Molecules* 19 (10): 16477–88. DOI: https://doi.org/10.3390/molecules191016477.

Li C. L. H., Wang Q., Zhou M., Li M., Gong T., Zhang Z., Sun X. (2017) pH-sensitive polymeric micelles for targeted delivery to inflamed joints. *Journal of controlled release:official journal of the Controlled Release Society* 246:133–141. DOI: https://doi.org/10.1016/j.jconrel.2016.12.027.

Liang-Peng W., Xin-jun L., Zhen-Hong Y., Yong C. (2009) The fabrication of TiO_2-supported zeolite with core/shell heterostructure for ethanol dehydration to ethylene. *Catalysis Communications* 11:67–70. DOI: https://doi.org/10.1016/j.catcom.2009.08.013.

Liquan H., Wen L., Yang L., Shouchun Y. (2023) Nanoparticle-based drug delivery systems targeting cancer cell surfaces. *RSC Adv.* 13:21365–21382. DOI: https://doi.org/10.1039/D3RA02969G.

Lu M., Huang L., Zhan S. (2023) pH-sensitive Nanoparticles for High Loading and Efficient Delivery of Doxorubicin. *J. Wuhan Univ. Technol.-Mat. Sci. Edit* 38:929–937. DOI: https://doi.org/10.1007/s11595-023-2779-0.

Maretto M., Blanchi F., Vignola R. (2014) Microporous and mesoporous materials for the treatment of wastewater produced by petrochemical activities. *Journal of Cleaner Production* 77:22–34. DOI: https://doi.org/10.1016/j.jclepro.2013.12.070.

Marlina A., Ginting N. B. (2015) Preparation and characterization of natural zeolite and rice husk ash as filler material in HDPE thermoplastic. *Chemistry and Materials Research* 7 (2): 20–29. http://www.iiste.org/journals

Mendoza-Castro M. J., Qie Z., Fan X., Linares N., García-Martínez J. (2023) Tunable hybrid zeolites prepared by partial interconversion. *Nature Communications* 14:1256–1260. DOI: https://doi.org/10.1038/s41467-023-36502-3.

Mingxia J., Wenqiang C., Wenjing Y., Zhiwei X., Xinyue L., Qingmiao J., Xiuwen G., Weifen Z., Weifen Z. (2021) Sequentially pH-Responsive Drug-Delivery Nanosystem for Tumor Immunogenic Cell Death and Cooperating with Immune Checkpoint Blockade for Efficient Cancer Chemoimmunotherapy. *ACS Appl. Mater. Interfaces* 13:43963–43974. DOI: https://doi.org/10.1021/acsami.1c10643.

Minotti G., Menna P., Salvatorelli E., Cairo G., Gianni L. (2004) Anthracyclines: molecular advances and pharmacologic developments in antitumor activity and cardiotoxicity. *Pharmacological Reviews* 56:185–229. DOI: https://doi.org/10.1124/pr.56.2.6.

Mirjalili F., Fakharpour M., Molahasanpour A. (2022) Investigating the effect of different percentages of surfactant and modifier on the microstructure and morphology of montmorillonite nanoparticles. *Journal of Ceramic Science and Engineering* 11:80–93. https://www.magiran.com/p2563809

Mosavi Fard A., Salehi F., Shariati A. (2013) Study of effective factors on synthesis of nano mordenite zeolite for use as a catalyst. *Journal of Applied Research in Chemistry (JARC)* 3:65–87.

Mosmann T. (1983) Rapid colorimetric assay for cellular growth and survival: application to proliferation and cytotoxicity assays. *Journal of Immunological Methods* 65:55–63. DOI: https://doi.org/10.1016/0022-1759(83)90303-4.

Mu X., Zhang M., Wei A. (2021) Doxorubicin and PD-L1 siRNA Co-delivery with Stem Cell Membrane-coated Polydopamine Nanoparticles for the Targeted hemoimmunotherapy of PCa Bone Metastases[J]. *Nanoscale* 13 (19): 8998–9008.

Nabiollah M., Navid R., Homayon A. (2013) Porosity, characterization and structural properties of natural zeolite–clinoptilolite as a sorbent. *Environment Protection Engineering* 39:139–151. DOI: https://doi.org/10.5277/EPE130111.

Naeej A., Mohseni A., Jafari A. (2012) Removal of nitrate from water by zero-valent iron. *Iranian Environmental Health Association Journal* 4:475–486.

Nik A., Alias M. (2007) Removal of Cr(III) from aqueous solutions using zeolite NaY prepared from rice husk ash. *The Malaysian Journal of Analytical Science* 11:76–83. https://api.semanticscholar.org/CorpusID:91690726

Nisi A., Babai A. (2014) Performance review of modified clinoptilolite zeolite by hexadecyltrimethylammonium chloride. *Rafsanjan Medical Journal* 15:343–354.

Ojo A. T., Ma C., Lee P. I. (2020) Elucidating the effect of crystallization on drug release from amorphous solid dispersions in soluble and insoluble carriers. *International Journal of Pharmaceutics* 591:120005. DOI: https://doi.org/10.1016/j.ijpharm.2020.120005.

Ordou N., Fathizadeh M. (2011) Controlling yield of NaY zeolite synthesis by hydrothermal method. *International Journal of Industrial Chemistry* 2:190–195.

Pandya T., Patel S., Kulkarni M., Singh Y. R., Khodakiya A., Bhattacharya S., Prajapati B. G. (2024) Zeolite-based nanoparticles drug delivery systems in modern pharmaceutical research and environmental remediation. *Heliyon* 10:e36417. DOI: https://doi.org/10.1016/j.heliyon.2024.e36417.

Rahman M., Awang M., Yuof A. (2012) Preparation, characterization and application of zeolite Y for water filtration. *Australian Journal of Basic and Applied Science* 6:50–54.

Rosas-Arbelaez W., Fijneman A. J. (2020) Friedrich H, Palmqvist AEC. Hierarchical micro-/mesoporous zeolite microspheres prepared by colloidal assembly of zeolite nanoparticles. *RSC Adv.* 10 (60): 36459–36466. DOI: https://doi.org/10.1039/d0ra07394f.

Rostami R., Jafari A., Kalantari R. (2012) Performance review of modified clinoptilolite zeolite and modified clinoptilolite by nano copper oxide. *Iranian Environmental Health Association Journal* 5:1–8.

Sharma P., Rajaram P., Tomar R. (2008) Synthesis and morphological studies of nanocrystalline MOR type zeolite material. *Journal of Colloid and Interface Science* 325:547–557. DOI: https://doi.org/10.1016/j.jcis.2008.05.058.

Shi J., Kantoff P. W., Wooster R., Farokhzad O. C. (2017) Cancer nanomedicine: progress, challenges and opportunities. *Nature reviews. Cancer* 17:20–37. DOI: https://doi.org/10.1038/nrc.2016.108.

Son D. C., Kieu Anh V. T., Thom N. T., Nguyen H. L. T., Hai L. V., Thien C. T., Hoang N. T., Lam T. D., Nam P. T., Trang N. T. T. (2023) Preparation and modification of zeolite A from kaolin for catalytic methanation of carbon dioxide. *Vietnam Journal of Chemistry* 61:170–177. DOI: https://doi.org/10.1088/1757-899X/1092/1/012094.

Song Z., Bi M., Li J. (2024) Synthesis of TiO_2-Modified Y Zeolite and its Adsorption-Catalytic Oxidative Desulfurization Performance. Silicon:4159–4172. DOI: https://doi.org/10.1007/s12633-024-02982-1.

Toshev L., Valitechev P. (2005) Nano zeolite synthesis, crystallization mechanism and application. *Chemistry of Materials* 17:2494–2513. DOI: https://doi.org/10.1021/cm047908z.

Vy Anh T. A., Sang-Wha L. (2021) pH-triggered degradation and release of doxorubicin from zeolitic imidazolate framework-8 (ZIF8) decorated with polyacrylic acid. *RSC Adv* 11:9222–9223.

Yaneri P., Petit D. (2013) Linde type A zeolite and type Y faujasite as a solid-phase for lead, cadmium, nickel and cobalt preconcentration and determination using a flow injection system coupled to flame atomic absorption spectrometry. *American Journal of Analytical Chemistry* 4:8–14. DOI: https://doi.org/10.4236/ajac.2013.48049.

Zhang L., Sujuan X., Wenjie L., Xiujie L., Shenglin X., Longya X. (2011) Crystallization and morphology of mordenite zeolite influenced by various parameters in organic-free synthesis. *Research Bulletin* 46:894–900.

Ziental D., Czarczynska-Goslinska B., Mlynarczyk D. T., Glowacka-Sobotta A., Stanisz B., Goslinski T., Sobotta L. (2020) Titanium Dioxide Nanoparticles: Prospects and Applications in Medicine. *Nanomaterials (Basel)* 10:387. DOI: https://doi.org/10.3390/nano10020387.